doi:10.1093/plphys/kiab120 PLANT PHYSIOLOGY 2021: 0: 1–16

Plant Physiology®

Research Article

# The protein kinase CPK28 phosphorylates ascorbate peroxidase and enhances thermotolerance in tomato

Zhangjian Hu,[1] Jianxin Li,[1] Shuting Ding,[1] Fei Cheng ,[1] Xin Li,[2] Yuping Jiang,[3] Jingquan Yu ,[1] Christine H. Foyer ,[4] and Kai Shi [1,5,*,†]

1 Department of Horticulture, Zhejiang University, Hangzhou 310058, China
2 Key Laboratory of Tea Quality and Safety Control, Ministry of Agriculture, Tea Research Institute, Chinese Academy of Agricultural Sciences, Hangzhou 310008, China
3 Department of Ecological Technology and Engineering, Shanghai Institute of Technology, Shanghai 201418, China
4 School of Biosciences, College of Life and Environmental Sciences, University of Birmingham, Edgbaston B15 2TT, UK
5 Zhejiang Provincial Key Laboratory of Horticultural Plant Integrative Biology, Hangzhou 310058, China

*Author for communication: kaishi@zju.edu.cn
†Senior author.

K.S. conceived the research; Z.H., J.Y., and K.S. designed the research; Z.H., J.L., and S.D. performed the experiments and analyzed the data; F.C. and X.L. provided technical support; Y.J. discussed interpretations with K.S.; Z.H., C.H.F., and K.S. wrote the article with contributions from other authors.
The author responsible for distribution of materials integral to the findings presented in this article in accordance with the policy described in the Instructions for Author (https://academic.oup.com/plphys) is: Kai Shi (kaishi@zju.edu.cn).

## Abstract

High temperatures are a major threat to plant growth and development, leading to yield losses in crops. Calcium-dependent protein kinases (CPKs) act as critical components of $Ca^{2+}$ sensing in plants that transduce rapid stress-induced responses to multiple environmental stimuli. However, the role of CPKs in plant thermotolerance and their mechanisms of action remain poorly understood. To address this issue, tomato (*Solanum lycopersicum*) *cpk28* mutants were generated using a CRISPR-Cas9 gene-editing approach. The responses of mutant and wild-type plants to normal (25°C) and high temperatures (45°C) were documented. Thermotolerance was significantly decreased in the *cpk28* mutants, which showed increased heat stress-induced accumulation of reactive oxygen species (ROS) and levels of protein oxidation, together with decreased activities of ascorbate peroxidase (APX) and other antioxidant enzymes. The redox status of ascorbate and glutathione were also modified. Using a yeast two-hybrid library screen and protein interaction assays, we provide evidence that CPK28 directly interacts with cytosolic APX2. Mutations in *APX2* rendered plants more sensitive to high temperatures, whereas the addition of exogenous reduced ascorbate (AsA) rescued the thermotolerance phenotype of the *cpk28* mutants. Moreover, protein phosphorylation analysis demonstrated that CPK28 phosphorylates the APX2 protein at Thr-59 and Thr-164. This process is suggested to be responsive to $Ca^{2+}$ stimuli and may be required for CPK28-mediated thermotolerance. Taken together, these results demonstrate that CPK28 targets APX2, thus improving thermotolerance. This study suggests that CPK28 is an attractive target for the development of improved crop cultivars that are better adapted to heat stress in a changing climate.

## Introduction

Increasing anthropogenic emissions have led to increasing and irreversible climate change. Consequently, global warming is generating a rapid increase in air temperatures that will have a profound impact on agriculture and natural ecosystems (Mittler and Blumwald, 2010). When heatwave

Received September 9, 2020. Accepted February 26, 2021. Advance access publication March 12, 2021

temperatures exceed critical thresholds, plant growth and development will be impeded as a result of decreased photosynthetic activity, disruption of plasma membrane integrity, protein denaturation, reduced enzyme capacities, and increased oxidative stress (Ohama et al., 2017; Vu et al., 2019). Plants have evolved multiple mechanisms to tolerate high-temperature stress, such as the induction of heat shock proteins (HSP) and the activation of antioxidant systems that scavenge reactive oxygen species (ROS) as well as regulated fluctuations in the levels of cytosolic $Ca^{2+}$ and altered stomatal development and movements (Mittler et al., 2012; Lamers et al., 2020). Together, these changes serve to minimize heat-induced inactivation of key processes.

High temperatures lead to the activation of specific membrane-localized calcium channels, which trigger a rapid $Ca^{2+}$ influx that activates downstream high temperature-stress responses (Mittler et al., 2012). Cytosolic $Ca^{2+}$ alterations are decoded via specific $Ca^{2+}$ sensors and associated signaling pathways. There are three major families of calcium sensors in terrestrial plants, including calmodulins (CaMs), calcineurin B-like (CBL) proteins, and calcium-dependent protein kinases (CPKs, also called as CDPKs; Boudsocq and Sheen, 2013). Of the $Ca^{2+}$ sensors, CPKs are unique because they function as $Ca^{2+}$ responders that catalyze the direct phosphorylation of downstream target substrates. Genome-wide exploration of *Arabidopsis thaliana*, rice (*Oryza sativa*), and tomato (*Solanum lycopersicum*) has revealed the presence of 34, 29, and 29 CPK genes, respectively (Cheng et al., 2002; Asano et al., 2005; Hu et al., 2016). CPKs are typically composed of four domains: an *N*-terminal variable domain, a Ser/Thr kinase domain, an auto-inhibitory junction region, and a regulatory calmodulin-like domain (Boudsocq and Sheen, 2013). At low cytosolic $Ca^{2+}$ concentration, the auto-inhibitory junction region restrains CPK activity and maintains the inactive status of the protein. Increasing $Ca^{2+}$ levels trigger conformational changes in the CPK proteins to release auto-inhibition and increase kinase activity (Christodoulou et al., 2004). A truncated variant of CPK that contains only the *N*-terminal variable domain and the kinase domain is constitutively active, even in the absence of a $Ca^{2+}$ influx (Monaghan et al., 2014).

A growing body of evidence indicates that CPKs are involved in environmental stress signaling upon the perception of external stimuli. In Arabidopsis, AtCPK5/6/11 were shown to be redundant positive regulators of plant immunity to *Pseudomonas syringae* pv. *tomato* DC3000 and *Botrytis cinerea* (Boudsocq et al., 2010; Dubiella et al., 2013; Gravino et al., 2015). Moreover, the *Atcpk8*, *Atcpk10*, and *Atcpk4/11* mutants were significantly impaired in ABA-mediated stomatal closure in response to drought stress (Zhu et al., 2007; Zou et al., 2010; Zou et al., 2015), whereas *Atcpk33* mutants were hypersensitive to ABA activation of stomatal closure, promoting drought tolerance (Li et al., 2016). The overexpression of rice *OsCDPK7* enhanced tolerance to multiple abiotic stresses, including cold, salinity, and drought (Saijo et al., 2000). In tomato, SlCPK27 is an essential regulator of cold tolerance via crosstalk with ROS and reactive nitrogen species (Lv et al., 2018). In contrast to other environmental stresses described above, the functions of CPKs in thermotolerance remain poorly characterized.

Several genome-wide expression studies have shown that multiple CPK isoforms are highly expressed in response to high-temperature stress. For example, the levels of transcripts encoding seven cucumber (*Cucumis sativus*) CsCPK isoforms, including *CsCDPK2/6/10/15*, were greatly increased in response to high-temperature treatments (Xu et al., 2015). Similarly, the abundance of transcripts encoding nine CaCDPK isoforms was greatly increased in response to heat stress in pepper (*Capsicum annuum*; Cai et al., 2015). Grapevine (*Vitis amurensis*) *VaCPK2/3/9/20/21/29* were identified as high temperature-responsive genes, and *VaCPK29* was further shown to be involved in the positive regulation of thermotolerance based on transient overexpression studies in *V. amurensis* callus cells (Dubrovina et al., 2013; Dubrovina et al., 2017). In tomato, 13 out of the 29 CPK isoforms were expressed in response to high-temperature stress, i.e., 45°C (Hu et al., 2016). In particular, the abundance of *CPK9/23/28* transcript was significantly increased within the first hour after high-temperature treatment (Hu et al., 2016). In an independent study, the accumulation of tomato *CPK28* (previously named *LeCPK2*) mRNAs was induced soon after exposure to high temperatures (Chang et al., 2009). Thus, it is reasonable to hypothesize that this tomato CPK28 functions as a $Ca^{2+}$ sensor in the regulation of thermotolerance.

Tomato is an economically important crop worldwide, as well as an established research model for the *Solanaceae*. Typically, the optimal temperatures for tomato growth are 20–25°C. High temperature (higher than 35°C) in greenhouse and field conditions negatively affect the vegetative and reproductive phases of tomato growth, particularly leading to a disruption of fruit set, which can result in losses of up to 70% at harvest (Ruggieri et al., 2019). To investigate the functions of *CPK28* in the control of thermotolerance in tomato, we generated stable tomato *cpk28* mutants via a CRISPR-Cas9 gene-editing approach. The characterization of these mutants demonstrates that this gene has a positive function in thermotolerance in tomato. We provide evidence that a cytosolic ascorbate peroxidase APX2 is a substrate of CPK28; the phosphorylation of Thr-59 and Thr-164 in the APX2 protein is potentially crucial to the regulation of this antioxidant enzyme and its associated metabolism in response to high-temperature stress. These findings not only create a step-change in our current understanding of the biological function of CPK28 in thermotolerance but also identify new targets and markers for the development of improved cultivars that are better equipped to combat heat stress.

## Results

### Loss-of-function of CPK28 impairs thermotolerance in tomato

We isolated two individual CRISPR-Cas9-edited lines for *CPK28* (*cpk28*#36 and *cpk28*#44). These carry 11-bp and

2-bp deletions in the first exon, respectively (Figure 1A). There were slight growth differences between the *cpk28* lines and the wild-type (WT) plants under optimal growth conditions. For example, both *cpk28* lines exhibited a small decrease in shoot height (Figure 1B, top panel). To investigate the role of CPK28 in thermotolerance, 4-week-old *cpk28* and WT plants were exposed to temperatures of 45°C. After a 12-h period of temperature treatment, the *cpk28* mutants displayed strikingly lower thermotolerance properties than the WT plants (Figure 1B). High-temperature stress led to a greater decline of the maximal efficiency of PSII (*Fv*/*Fm*) in both *cpk28* lines, whereas the *Fv*/*Fm* values were not changed as a result of the normal-temperature treatment in any of the lines (Figure 1C). Electrolyte leakage was significantly increased as a result of the high-temperature treatment in the *cpk28* lines and the malondialdehyde (MDA) levels were increased (Figure 1, D and E). Taken together, these results demonstrated that CPK28 plays a positive role in thermotolerance in tomato.

CPK28 is a high-affinity, $Ca^{2+}$ binding protein and its activity are dependent on the availability of $Ca^{2+}$ signals (Bender et al., 2017). We, therefore, determined the role of $Ca^{2+}$ availability in thermotolerance. The chlorophyll contents of leaf discs supplemented with different concentrations of $CaCl_2$ were higher following high-temperature stress than that in control discs supplemented only with equivalent concentrations of KCl. The discs supplemented with 40 mM $CaCl_2$ showed the greatest heat-stress tolerance (Supplemental Figure S1, A and B).

## High temperature-induced ROS accumulation and protein oxidation is aggravated in the *cpk28* mutants

High-temperature stress usually leads to oxidative stress via the overproduction of ROS (Choudhury et al., 2017). To determine the role of CPK28 in the control of high temperature-induced oxidation, we first evaluated the accumulation of $H_2O_2$ using DAB staining and $O_2^{\bullet-}$ accumulation using NBT staining (Figure 2, A and B). The observed increase in brown and blue staining, respectively, indicated the high-level accumulation of these oxidants in the leaves exposed to high temperatures (Figure 2, A and B). Consistent with the histochemical staining, quantification of leaf $H_2O_2$ levels confirmed that $H_2O_2$ contents were higher in the *cpk28* mutants than in the WT plants following the high-temperature treatment (Figure 2C).

Temperature causes conformational changes to proteins and directly influences protein abundance and turnover. To determine the effects of CPK28 on high-temperature-dependent effects on protein properties, we measured the carbonylation state of leaf proteins using 2,4-dinitrophenol (DNP) and anti-DNP antibodies in the *cpk28* and WT plants after high-temperature treatment. As shown in Figure 2D, *CPK28* loss of function led to a greater temperature-dependent increase in the level of protein carbonylation, whereas the *cpk28* and WT control plants showed similar levels of oxidized proteins under normal temperatures. The molecular chaperone HSP70 regulates protein quality by renaturing heat-denatured proteins (Hahn et al., 2011). Similarly, APX and 2-Cys peroxiredoxins (2-CP) are ROS-scavenging proteins, associated with cellular redox regulation (Awad et al., 2015). The high temperature-induced increases in the HSP70 protein, as detected by specific antibodies, were similar in the *cpk28* and WT plants (Figure 2E). In contrast, the heat-induced increase in the levels of the cytosolic APX protein was largely suppressed in the *cpk* 28 plants, and the levels of the 2-CP monomer were deceased more in the *cpk* 28 lines than the WT plants in response to high-temperature stress (Figure 2E). The monomer form of 2-CP has the greatest peroxidase enzyme (Jang et al., 2004). Taken together, these results show that the heat stress-induced regulation of cellular redox homeostasis was disrupted in the *cpk28* lines.

## Regulation of cellular redox homeostasis is downstream of CPK28 in thermotolerance

The activation of antioxidant enzymes such as APX, catalase (CAT), dehydroascorbate reductase (DHAR), and glutathione reductase (GR) protect against temperature-induced ROS accumulation (Cheng et al., 2016). The high temperature-induced increase in the activities of these antioxidant enzymes was significantly compromised in both *cpk28* lines compared to the WT (Figure 3A). Moreover, the loss of *CPK28* functions led to a slight decrease in the activities of APX at the normal temperature (Figure 3A). Additionally, both ascorbate and glutathione are abundant and stable antioxidants, acting as the heart of the cytosol redox hub with appropriate redox potentials (Foyer and Noctor, 2011). Shifts in reduced ascorbate to dehydroascorbate (AsA/DHA) and reduced glutathione to glutathione disulfide (GSH/GSSG) ratios are generally accepted as indicators of changes in redox status (Foyer and Noctor, 2011). The total amounts of the ascorbate (AsA plus DHA) and glutathione (GSH plus GSSG) pools were similar in all lines irrespective of the temperature regime (Figure 3B). Whereas AsA/DHA ratios were lower in the *cpk28* mutants than in the WT plants at both temperatures, GSH/GSSG ratios were lower in the *cpk28* mutants than in the WT plants after the high-temperature treatment but not under normal temperatures (Figure 3C).

We then tested whether the thermotolerance in *cpk28* plants could be increased by the application of exogenous AsA. Exogenous AsA treatments alleviated the high temperature-induced wilting of the *cpk28* lines, which thereafter showed similar changes to the WT controls (Figure 4, A and B). An analysis of the ascorbate content and the redox state of the ascorbate pool was performed after exogenous AsA treatment (Figure 4C). The application of AsA increased the endogenous AsA contents of all lines without any significant changes in the DHA contents (Figure 4D) under both normal and high temperatures. As the consequence, the AsA/DHA ratios were significantly increased, especially in the *cpk28* mutants, leading to enhanced thermotolerance at high temperatures (Figure 4E). Therefore, ascorbate

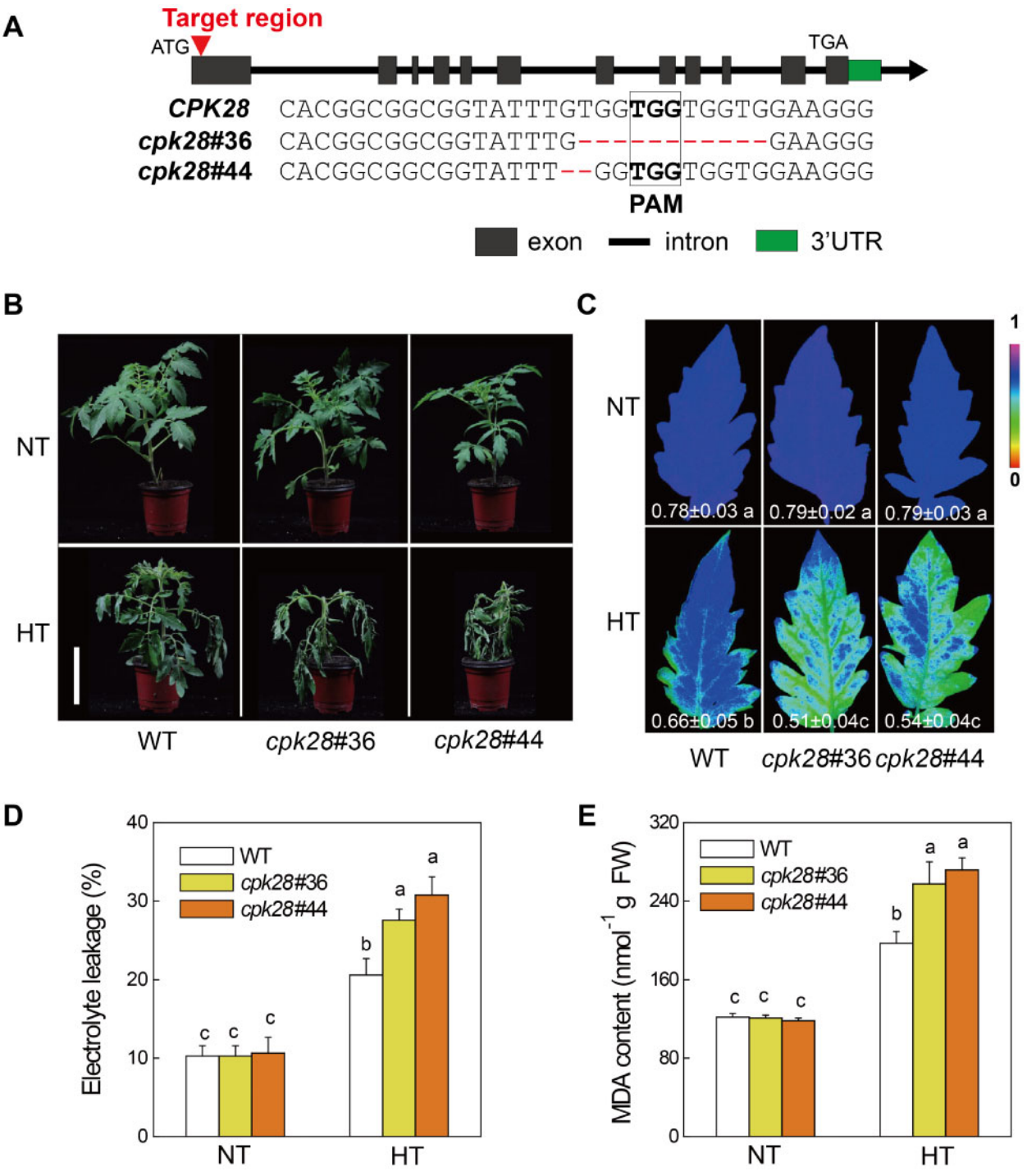


**Figure 1** Role of *CPK28* gene in tomato thermotolerance. A, Schematic illustration of the sgRNA target site (red arrows) in wild type (WT) *CPK28* and two alleles (*cpk28#36* and *cpk28#44*) from CRISPR-Cas9 T2 mutant lines. Red font presents the deletion sequences, and black box presents protospacer-adjacent motif (PAM) sequences. B, Representative images of *cpk28* mutant and WT plants. Bar = 10 cm. The *cpk28* and WT plants were subjected to normal temperature (NT, 25°C) or high temperature (HT, 45°C) treatment, and the plant images were taken 12 h later. C, The representative leaf images indicating the maximum photochemical efficiency of photosystem II (*Fv*/*Fm*) after 7 h of different temperature treatments. The color gradient scale at the bottom indicates the magnitude of the fluorescence signal represented by each color. D, The relative electrolyte leakage of tomato leaves after 7 h of different temperature treatments. E, The accumulation of the membrane lipid peroxidation product MDA in tomato leaves after 7 h of different temperature treatments. Images shown in B and C were digitally extracted and scaled for comparison. The data in C to E are presented as mean values ± SD; $n = 3$. Different letters indicate significant differences between treatments ($P < 0.05$, Tukey's test).

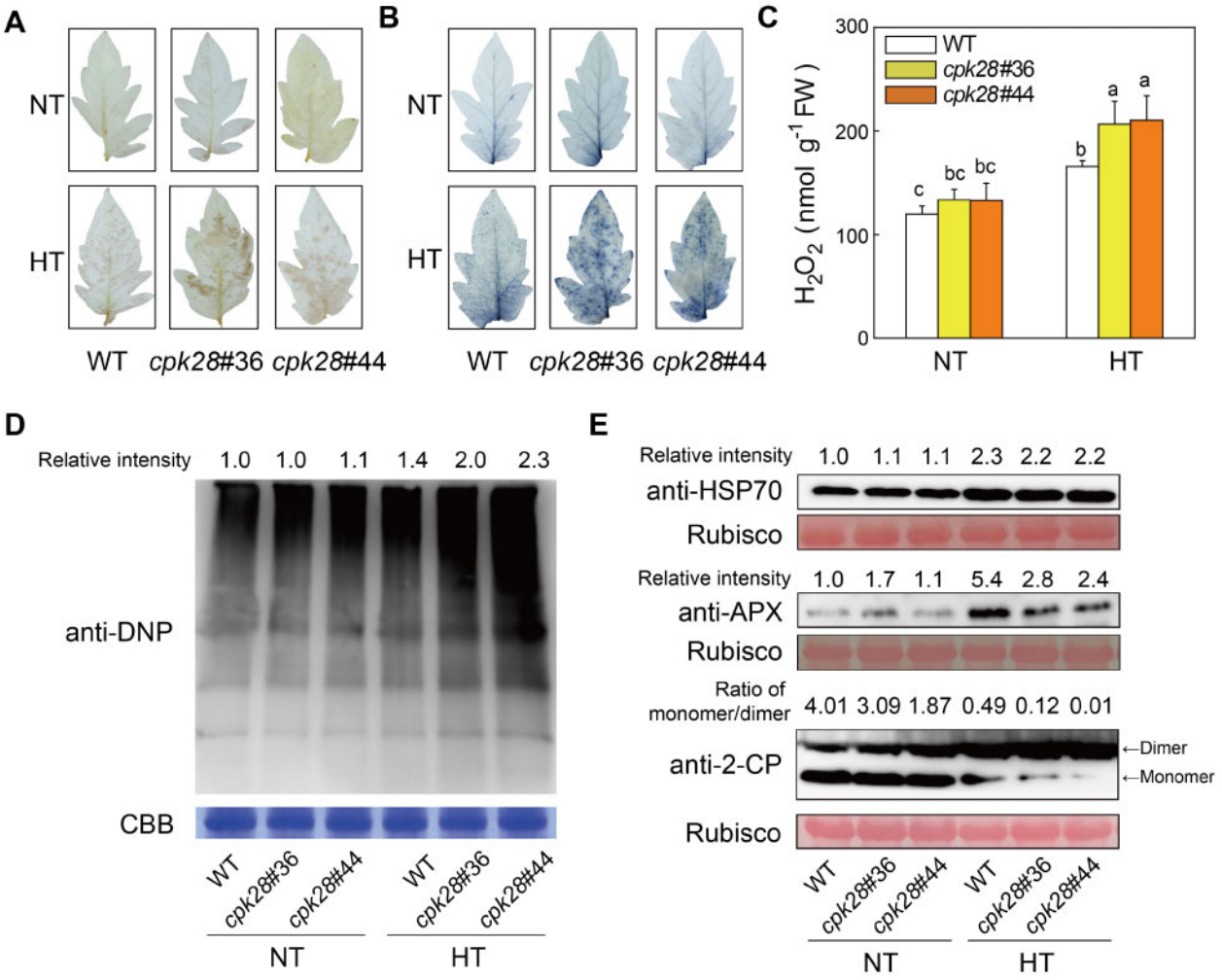


**Figure 2** Response of ROS accumulation and protein oxidation to high temperature in *cpk28* mutants. A, Representative images of $H_2O_2$ accumulation as determined by DAB staining. B, Representative images of $O_2^-$ accumulation as determined by NBT staining. The *cpk28* and wild type (WT) plants were subjected to normal-temperature (NT, 25°C) or high-temperature (HT, 45°C) treatment, and leaf samples were collected 7 h later. C, Quantification of $H_2O_2$. Leaf samples were collected 7 h after different temperature treatments. D, Oxidation of soluble proteins were detected by immunoblot analysis with anti-DNP antibody. Leaf samples were collected 7 h after different temperature treatments. The soluble proteins from leaf were isolated and derivatized by 2,4-dinitrophenol (DNP). The protein input was indicated by Coomassie Blue staining (CBB), and the relative intensity of oxidative protein was labeled on the top of the image. E, Immunoblot analysis of the protein abundance of HSP70 and cytosolic APX, and protein conformational change of 2-CP. Leaf samples were collected 7 h after different temperature treatments. The protein input was indicated by Ponceau S staining of Rubisco. Images shown in A and B were digitally extracted and scaled for comparison. The data are presented in C as mean values ± SD; $n = 4$. Different letters indicate significant differences between treatments ($P < 0.05$, Tukey's test).

metabolism appears to function downstream of CPK28 in thermotolerance.

## CPK28 directly targets cytosolic APX2 and this interaction is responsive to $Ca^{2+}$ stimuli

We next identified CPK28-interacting proteins to gain better insights into the mechanisms of CPK28-mediated effects on cellular redox homeostasis and thermotolerance. We performed a yeast two-hybrid (Y2H) screen with baits comprised of the variable *N*-terminal domain and the kinase domain of CPK28 (referred to as CPK28VK), which is regarded as a constitutively active variant of CPK28 (Monaghan et al., 2014). Of the 100 or so candidate CPK28-interacting proteins that were identified (Supplemental Table S1), one clone encoding a cytosolic APX2 (Solyc06g005150.2.1) was confirmed to have strong interaction with CPK28 in Y2H and GST pull-down assays (Figure 5, A and B). BiFC assay showed the CPK28–APX2 complex is mainly present in the cytosol (Figure 5C). *In planta* split-luciferase (split-Luc) assays and co-immunoprecipitation (Co-IP) assays further demonstrated that the intensity of the CPK28–APX2 interaction was enhanced in the presence of exogenous $Ca^{2+}$, and *vice versa* it was inhibited in the presence of the exogenous $Ca^{2+}$ chelator, EGTA (Figure 5, D and E).

To further investigate the functions of *APX2* in response to high-temperature treatments, we generated *apx2* mutants via CRISPR-Cas9-mediated gene editing, and isolated two stable lines, *apx2*#2 and *apx2*#4, which contained 1-bp

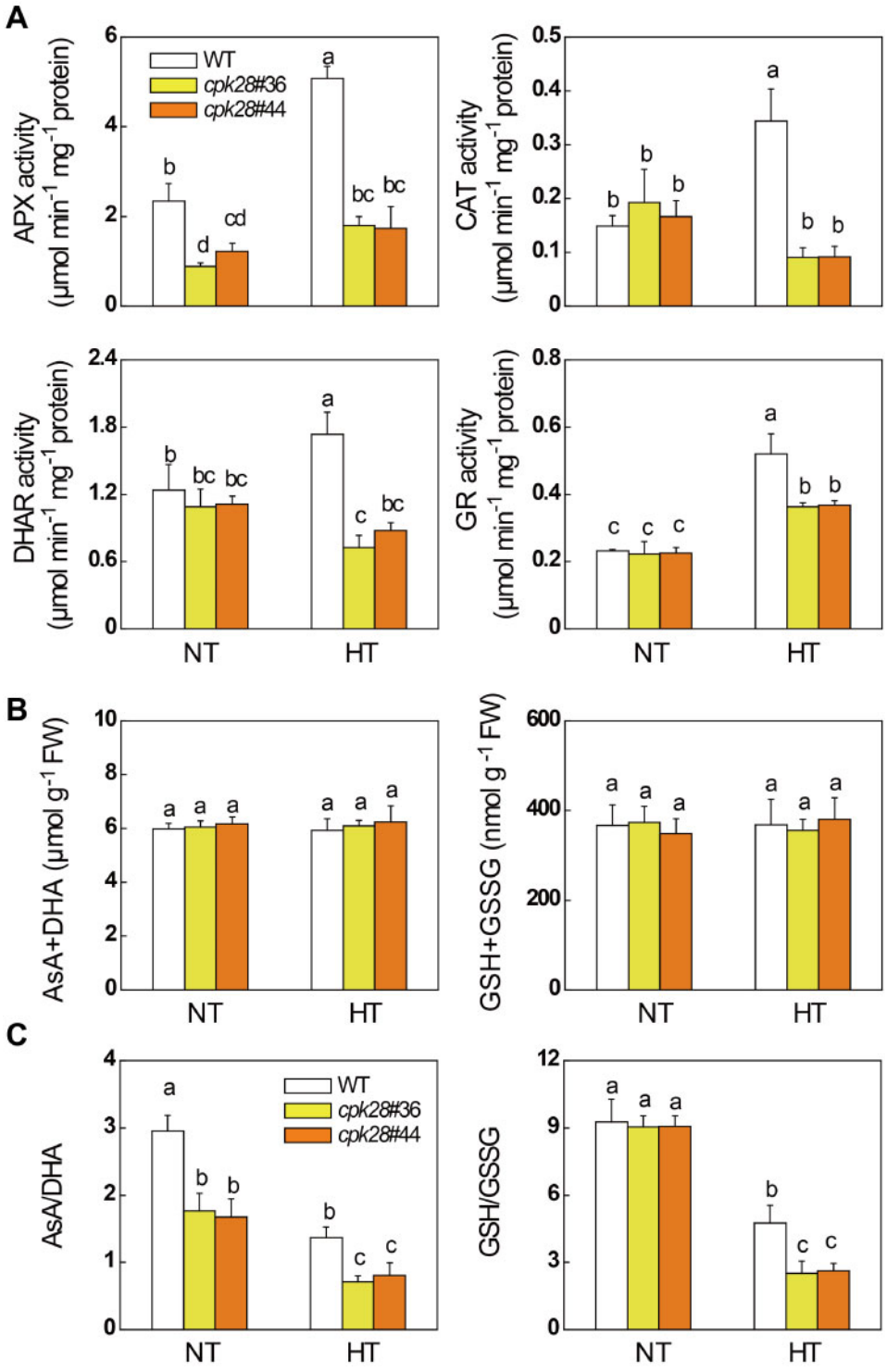


**Figure 3** The changes of antioxidants and enzyme activities in response to high temperature in *cpk28* mutants. A, Effects of high-temperature treatment on antioxidant enzyme activities in *cpk28* mutants and wild-type (WT) plants. APX, ascorbate peroxidase; CAT, catalase; DHAR, dehydroascorbate reductase; GR, glutathione reductase. B, Effects of high-temperature treatment on ascorbate and glutathione contents. AsA, reduced ascorbate; DHA, dehydroascorbate; GSH, glutathione; GSSG, glutathione disulfide. C, Effects of high-temperature treatment on the redox statuses of ascorbate and glutathione. The *cpk28* mutants and WT plants were subjected to normal-temperature (NT, 25°C) or high-temperature (HT, 45°C) treatment, and leaf samples were collected 7 h later for enzyme activity and antioxidant content analysis. The data are presented as mean values ± SD; $n = 3$. Different letters indicate significant differences between treatments ($P < 0.05$, Tukey's test).

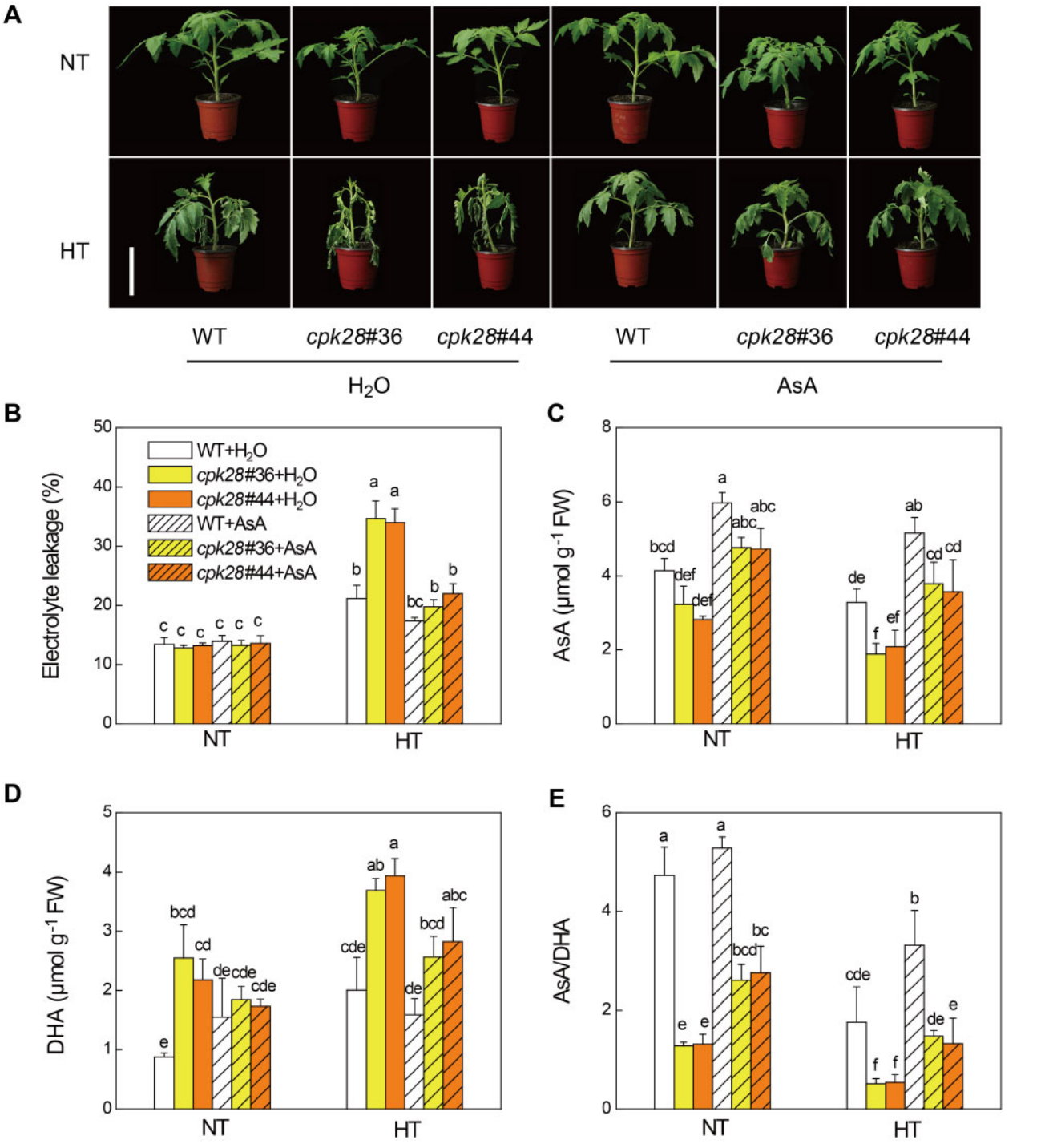


**Figure 4** Exogenous AsA treatment rescues *cpk28* mutants from high-temperature stress. A, Representative images of tomato plants as influenced by AsA and high-temperature treatment. The *cpk28* mutants and WT plants were pre-treated with 10 mM AsA and $H_2O$ control once per day for three successive days. Then, plants were subjected to normal temperature (NT, 25°C) or high temperature (HT, 45°C), and the plant images were taken 12 h later. Bar = 10 cm. Images shown were digitally extracted and scaled for comparison. B, The relative electrolyte leakage of tomato leaves after 7 h of different temperature treatments with or without AsA pretreatment. C–E, Effects of exogenous AsA treatment on the endogenous AsA content (C), DHA content (D), and its redox status (E) in *cpk28* and wild-type (WT) plants after 7 h of normal-temperature or high-temperature treatment. The data are presented in B–E as mean values ± SD; $n = 3$. Different letters indicate significant differences between treatments ($P < 0.05$, Tukey's test).

insertions of A and C in the fifth exon, respectively (Figure 6A). Compared with the WT plants, *apx2* mutants exhibited a significant reduction in thermotolerance after a 12-h exposure to high-temperature stress (Figure 6B). Moreover, the *apx2* mutants exhibited about 40% lower APX activities than the WT plants under normal

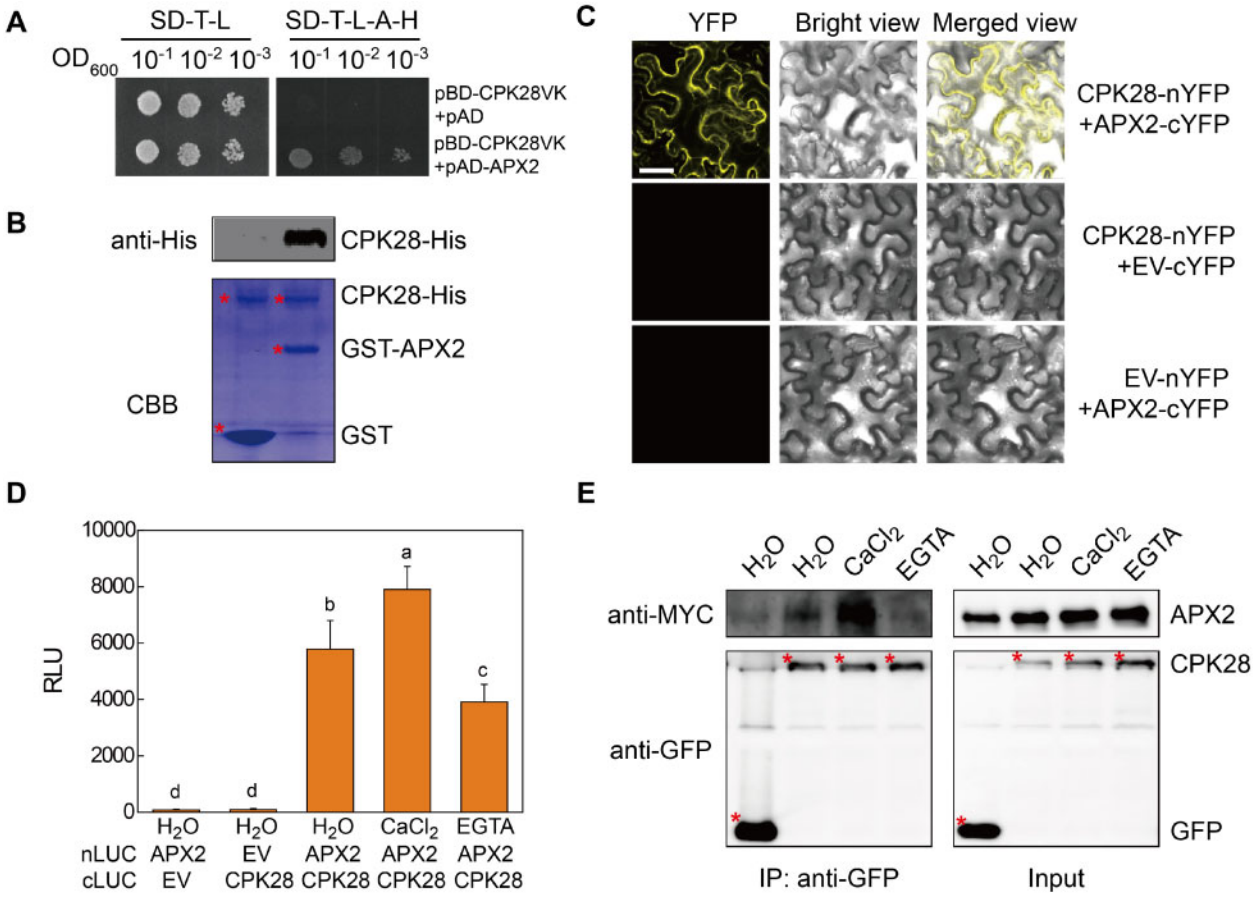


**Figure 5** CPK28 interacts with APX2, which was enhanced by $Ca^{2+}$ stimuli. **A,** Y2H assay shows interactions between CPK28VK and APX2. Protein–protein interactions were evaluated by the different concentration of yeast cells growth on selective media lacking Trp (T), Leu (L), Ade (A), and His (H). CPK28VK, a constitutively active variant of CPK28. **B,** GST pull-down assay of interactions between CPK28 and APX2 *in vitro*. GST or GST-APX2 immobilized on glutathione Sepharose beads was incubated with CPK28-His purified proteins. The beads were collected for immunoblotting with an anti-His antibody (top). The input fusion proteins were indicated by Coomassie brilliant blue (CBB) staining (bottom). The asterisks indicate proteins labeled on the right. **C,** BiFC analysis shows that CPK28–APX2 interaction occurs at the cytoplasm. Spliced YFP fusion constructs were transiently coexpressed in *N. benthamiana* leaves for 2 d. The YFP fluorescence signals were obtained by the confocal microscopy. Scale bar = 50 μm. **D,** Split-LUC assay and **E,** Co-IP assay show that CPK28–APX2 interaction is responsive to $Ca^{2+}$ stimuli. Indicated binary constructs were co-expressed in *N. benthamiana* transient expression system. 2 d later, the leaves were inoculated of 15 mM $CaCl_2$, 1.5 mM EGTA, or $dH_2O$ control just 1 h before sample collection. The relative luminescence units (RLU) and the APX2 protein abundance after GFP-agarose-mediated immunoprecipitation indicate levels of protein–protein interactions in split-LUC assay and Co-IP assay, respectively. The asterisks indicate proteins labeled on the right. The data are presented in **D** as mean values ± SD; $n = 8$. Different letters indicate significant differences between treatments ($P < 0.05$, Tukey's test).

temperatures, and they were unable to increase APX activities at high temperatures (Figure 6C). Thus, APX2 also appeared to be essential for the thermotolerance traits of tomato.

## Phosphorylation of APX2 by CPK28 at Thr-59 and Thr-164 sites is important for thermotolerance

We next assessed whether CPK28 induces phosphorylation of the APX2 protein. A GST-CPK28 fusion recombinant protein was shown to phosphorylate a His-APX2 substrate, based on immunoblotting with anti-phospho-serine/threonine (anti-pSer/pThr) and anti-phospho-threonine (anti-pThr) antibodies (Figure 7A). When CPK28 and APX2 were co-expressed in *N. benthamiana* leaves, the phosphorylation level of APX2 was significantly increased, and it was further increased in response to $Ca^{2+}$ stimuli (Figure 7B).

To identify the CPK28-mediated phosphorylation sites of APX2, the phosphorylated recombinant APX2 protein (produced by CPK28) was subjected to LC–MS/MS analysis. Two APX2 phospho-peptides incorporating the Thr-59 and Thr-164 sites were found to be phosphorylated by CPK28 (Figure 7, C and D). Both Thr sites are highly conserved in cytosolic APXs in tomato and Arabidopsis (Supplemental Figure S2), which implies that these phosphorylation events might also occur in other plant species. We then generated the threonine (T)-to-alanine (A) point mutant variants in APX2 ($APX2^{T59A}$, $APX2^{T164A}$, and $APX2^{T59A/164A}$), which are designed to block its phosphorylation within these two sites

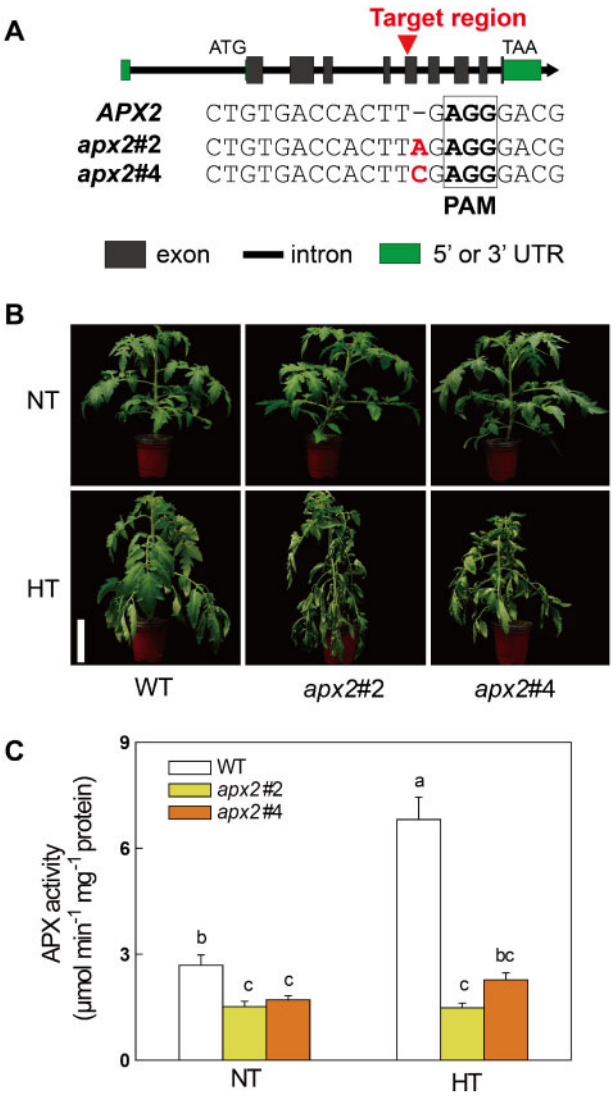


**Figure 6** Role of *APX2* gene in tomato thermotolerance. A, Schematic illustration of the sgRNA target site (red arrows) in wild type (WT) *APX2* and two alleles (*apx2*#2 and *apx2*#4) from CRISPR-Cas9 T2 mutant lines. Red font indicates inserted nucleotides, and black box presents protospacer-adjacent motif (PAM) sequences. B, Representative images of *apx2* lines after 12 h of normal-temperature (NT, 25°C) or high-temperature (HT, 45°C) treatment. Bar = 10 cm. Images shown were digitally extracted and scaled for comparison. C, Effects of high-temperature treatment on APX activities in *apx2* mutants and WT plants. The data are presented in C as mean values, and ± SD; $n = 8$. Different letters indicate significant differences between treatments ($P < 0.05$, Tukey's test).

by CPK28. Different site-directed APX2 mutants substantially reduced CPK28-mediated phosphorylation *in planta* (Figure 7E). To investigate the significance of these phosphorylation events in thermotolerance, the different site-directed mutants and WT APX2 variants were transiently overexpressed in the tomato *apx2* background (Supplemental Figure S3). The plants were then subjected to high-temperature treatment. Compared to the overexpression of the WT APX, the plants that overexpressed the site-directed mutants of APX exhibited lower *Fv*/*Fm* values and APX activity (Figure 7, F and G). Interestingly, $APX2^{T59A/164A}$ overexpression plants showed a similar level of thermotolerance to that observed in the YFP overexpressing control lines (Figure 7F). Because the site-directed mutation of APX caused significantly decreased APX activity *in vitro* (Figure 7H), this experiment on its own does not provide evidence for or against the role of APX phosphorylation in thermotolerance, which needs further investigation.

## Discussion

As $Ca^{2+}$ sensors, CPKs have been conserved during evolution; they are found in photosynthetic organisms ranging from green algae to vascular plants. These enzymes play critical roles in the regulation of plant responses to multiple environmental stimuli such as drought, salt, and chilling stresses (Zou et al., 2010; Campo et al., 2014; Zou et al., 2015; Li et al., 2016; Liu et al., 2018; Lv et al., 2018; Zhang et al., 2020). However, little is known about the functions of CPKs in thermotolerance, and the mechanisms of targeted CPK phosphorylation are poorly characterized. In this study, we present several lines of evidence supporting the conclusion that the tomato CPK28 mediates thermotolerance by phosphorylation of APX2, which in turn regulates cellular redox homeostasis in tomato.

### CPK28 increases thermotolerance in tomato

As discussed previously, several CPK genes are highly expressed in response to high temperatures, but their precise roles are unclear. Here, we show that CPK28 increases thermotolerance, as demonstrated by the loss of photosystem and cellular membrane functions in the *cpk28* mutants (Figure 1). In agreement with this conclusion, heterologous overexpression of *VaCPK29* was shown to enhance the high-temperature tolerance of Arabidopsis (Dubrovina et al., 2017). In another heterologous overexpression system, tea (*Camellia sinensis*) *CsCDPK20* and *CsCDPK26* were overexpressed in Arabidopsis, leading to improved thermotolerance by increasing the expression of stress-responsive genes, such as *AtAPX1* and *AtPOD* (Wang et al., 2018). Given that a previous study had shown that high temperature induces the expression of multiple CPK genes (Hu et al., 2016), it is possible that other CPK isoforms also contribute to thermotolerance; however, future studies are required to elucidate this point.

### CPK28 mediates thermotolerance through redox homeostasis changes

High-temperature stress is usually accompanied by the accumulation of ROS and alterations in protein stability and turnover (Mittler et al., 2012). HSPs and antioxidant enzymes are high temperature-responsive proteins that protect enzyme functions against the negative impacts of high-temperature stress (Ohama et al., 2017). The data presented here show that high-temperature stress-induced ROS accumulation and protein oxidation in tomato, factors that were

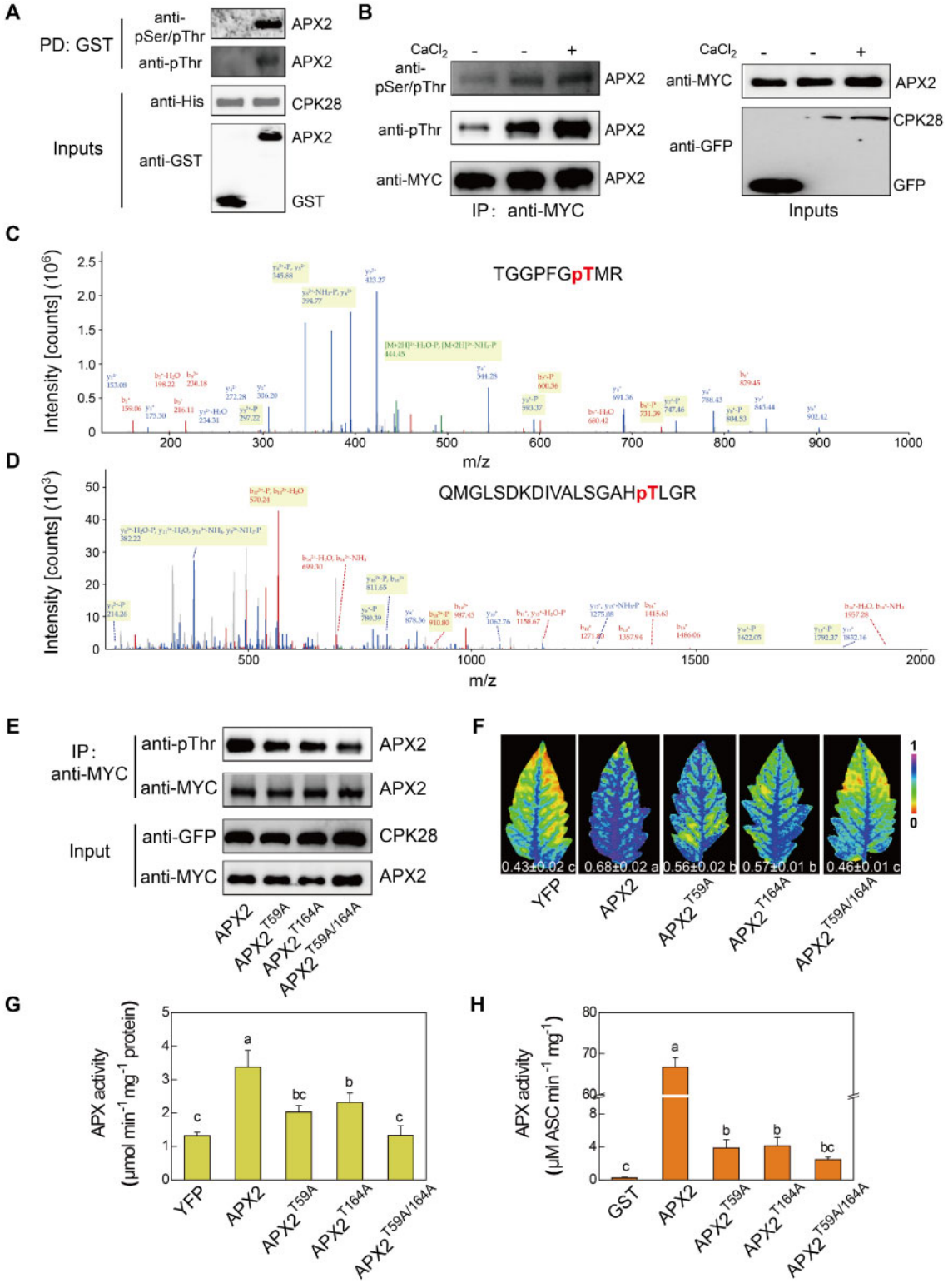


**Figure 7** Blocking the phosphorylation of APX2 at Thr-59 and Thr-164 sites by CPK28 inhibits tomato thermotolerance. A, CPK28 phosphorylates APX2 *in vitro*. The phosphorylation reactions were performed using His-CPK28 as the kinase and GST-APX2 as the substrate. After separation by SDS-PAGE, the phosphorylated APX2 protein was detected by anti-pSer/pThr and anti-pThr antibodies. B, $Ca^{2+}$ induces the phosphorylation of APX2 by CPK28 *in vivo*. Indicated binary constructs were co-expressed in *N. benthamiana* transient expression system. 2 d later, the leaves were inoculated with 15 mM $CaCl_2$ or $dH_2O$ control just 1 h before sample collection. The phosphorylated APX2 proteins were immunoprecipitated by the anti-MYC agarose beads (IP: anti-MYC), and then immunoblotted with anti-pSer/pThr and anti-pThr antibodies. C–D, The Thr-59 (C) and Thr-164 (D) residues of APX2 are phosphorylated by CPK28. An LC–MS/MS analysis of the phosphorylation reaction carried by His-CPK28 and GST-APX2 showed that the phosphorylation of Thr-59 and Thr-164 in APX2 by CPK28. The phosphorylated Thr residues in the APX2 fragment

further increased in the *cpk28* plants (Figure 2). Whereas the heat-induced accumulation of HSP70 protein was similar in all lines, accumulation of the cytosolic APX protein and the monomeric form of 2-CP were decreased in the *cpk28* plants compared to the WT in response to high-temperature stress (Figure 2E), suggesting a link between CPK28 and cellular redox homeostasis.

The AsA-GSH pools and ROS-scavenging enzymes regulate cellular redox homeostasis and prevent excessive ROS accumulation in response to high-temperature stress (Noctor et al., 2016). The activities of ROS-scavenging enzymes, especially APX, were found to be lower in *cpk28* plants than in WT under both temperature conditions (Figure 3A). APX has a high affinity for $H_2O_2$ ($K_m$ around 20–50 μM) and functions as a major ROS-scavenging enzyme in plants (Queval et al., 2008). As the specific electron donor for APX, AsA is at the center of the cellular redox hub, functioning to reduce $H_2O_2$ to water (Foyer and Noctor, 2011; Smirnoff and Arnaud, 2019). The data presented here show that loss of function of *CPK28* results in lower AsA/DHA ratios under both temperature conditions (Figure 3C). Consistent with these findings is the observation that maize (*Zea mays*) ZmCPK11 is involved in the regulation of ABA-induced antioxidant defenses by activating the activities of APX and SOD (Ding et al., 2013). Moreover, treatment with exogenous AsA enhanced endogenous AsA accumulation, leading to increased AsA/DHA ratios of the *cpk28* mutants to similar values as those observed in the WT control plants (Figure 4). This increased the protection of the *cpk28* plants against high-temperature stress and resulted in a similar level of thermotolerance as that observed in the WT controls (Figure 4). Earlier studies have shown that the exogenous application of AsA increases endogenous AsA accumulation and prevents oxidative stress-induced changes in leaves (Zheng et al., 2000; Maddison et al., 2002; Athar et al., 2008). Taken together, these findings suggest that the antioxidant system, and the APX-AsA module, in particular, functions downstream of CPK28-mediated thermotolerance.

## CPK28 phosphorylates APX2, thus improving thermotolerance

The identification and functional characterization of CPK28 substrates are critical to understand the molecular basis of CPK28-mediated thermotolerance in tomato. Earlier studies had identified several potential CPK substrates that are involved in redox-mediated, abiotic-stress responses, which transduce CPK-mediated signals that are initiated by $Ca^{2+}$ (Zou et al., 2015; Liu et al., 2018). A Y2H screen library was used to identify several candidates associated with redox homeostasis that bind to CPK28, including FRX, GRX, and APX2 (Supplemental Table S1). Of these candidates, the CPK28–APX2 interaction was confirmed using multiple *in vivo* and *in vitro* assays (Figure 5). Like the *cpk28* mutants, the *apx2* mutants were more sensitive to high-temperature stress than the WT (Figure 6). APX2 belongs to the cytosolic APX family, which exhibits responses to multiple abiotic stresses (Fryer et al., 2003; Rossel et al., 2006). A previous study in Arabidopsis showed that *AtAPX2* loss of function results in a higher level of high temperature-induced inhibition of root growth compared to WT plants (Suzuki et al., 2013).

The data presented here show that APX2 is potentially phosphorylated by CDPK28 at the Thr-59 and Thr-164 sites, as the analysis showed that a Thr-to-Ala point mutation at both sites significantly decreased thermotolerance responses (Figure 7). Notably, the CPK28–APX2 interaction and the phosphorylation state of the APX2 protein were shown to be responsive to $Ca^{2+}$ availability (Figures 5, D and E, 7B). In agreement with this finding, the role of $Ca^{2+}$ in the control of CPK-mediated interactions and the phosphorylation of target proteins was shown to be central to $Ca^{2+}$-initiated signaling transduction in multiple stress responses (Zou et al., 2015; Liu et al., 2018; Zhou et al., 2020). Arabidopsis AtCPK8 specifically targets another antioxidant enzyme, AtCAT3, and catalyzes the phosphorylation of the CAT protein at Ser-261, promoting an increase in catalase activity in the ABA-mediated regulation of stomatal closure during drought stress (Zou et al., 2015). By contrast, rice OsCPK24 phosphorylates OsGrx10, leading to an inhibition of activity in response to cold stress (Liu et al., 2018). Here, we should be more circumspect in interpreting the data indicating lower APX activities in Thr-to-Ala point-mutation lines (Figure 7, G–H), as reduced activity might not only be caused by a lack of phosphorylation sites, but also possibly because that the mutations have eliminated APX activity due to other disruptions. Also, future studies on the roles of CPKs in the regulation of the antioxidant system and its responses to heat stress will undoubtedly

are highlighted in red. E, Site-directed mutation of Thr residues in APX2 inhibited its phosphorylation by CPK28. The wild-type (WT) and Thr-mutated forms of APX2-MYC were co-expressed with CPK28-GFP in *N. benthamiana* leaves. The APX2 proteins were immunoprecipitated by anti-MYC agarose beads (IP: anti-MYC), and then analyzed by anti-pThr and anti-MYC antibodies. The protein inputs were indicated by immunoblotting. F, Effect of phospho-dead APX2 variants on thermotolerance in tomato *apx2* mutants. Agrobacterium carried with indicated binary vectors were transiently expressed in tomato *apx2* mutants for 2 d. After 12 h of high-temperature stress treatment at 45°C, samples were collected for representative leaf images indicating the maximum photochemical efficiency of photosystem II (*Fv*/*Fm*). The color gradient scale at the right indicates the magnitude of the fluorescence signal represented by each color. Images shown were digitally extracted and scaled for comparison. G, Effect of phospho-dead APX2 variants on APX activity in tomato *apx2* mutants. Indicated binary vectors were transiently expressed in tomato *apx2* mutants for 2 d, and the plants were subjected to high temperature (45°C) for 7 h before enzyme activity analysis. H, Blocking the phosphorylation of Thr-59 and Thr-164 sites of APX2 impaired APX activity *in vitro*. Purified recombinant GST-APX2, GST-APX2$^{T59A}$, GST-APX2$^{T164A}$, GST-APX2$^{T59A/T164A}$, and GST control protein were used for the enzymatic activity analysis. The data are presented in F to H as mean values ± SD; $n = 3$. Different letters indicate significant differences between treatments ($P < 0.05$, Tukey's test).

further our understanding of how these enzymes modulate thermotolerance.

In summary, the data presented here reveal a function for CPK28 in the regulation of thermotolerance, together with a molecular mechanism leading to the modulation of cellular redox homeostasis. This study not only highlights the importance of CPK28 but also points to new targets for plant improvement and stress management in response to a changing climate.

## Materials and methods

### Plant material, growth condition, and high-temperature treatment

Tomato (*Solanum lycopersicum* cv Condine Red) and *Nicotiana benthamiana* were used as wild type (WT) in this study. Tomato CRISPR-Cas9-edited lines of *cpk28* and *apx2* were generated with *Agrobacterium tumefaciens*-mediated cotyledon tissue culture as described previously (Hu et al., 2021). Seeds were sowed in pots filled with a mixture of peat and vermiculite (7:3, v/v) and receiving Hoagland nutrient solution. The growth conditions were maintained as follows: 14 h/10 h (day/night) photoperiod, 25°C/20°C (day/night) ambient air temperature, 400 μmol $m^{-2}$ $s^{-1}$ photosynthetic photon flux density.

Approximately 5-week-old plants were used for high-temperature treatments in growth chambers (Qiushi, China). For AsA pretreatment assay, the *cpk28* mutants and WT plants were sprayed with 10 mM AsA or $H_2O$ control once per day for three successive days. For *in planta* high-temperature treatments, tomato CRISPR-Cas9-edited lines and WT plants were exposed to high temperature (45°C) or control normal temperature (25°C). Other environmental parameters except temperature in the growth chambers were the same as previously described growth conditions. After 7 h of differential temperature treatments, pooled samples, with each sample being from two individual plants, were collected for the next assays. Representative plant images were taken after 12 h of differential temperature treatments. For *in vitro* high-temperature treatments, 1-$cm^2$ leaf discs detached from fourth fully expanded tomato leaves were floated in the indicated solutions and incubated at 45°C of 2 h for tomato, followed by recovery at 25°C for 2 d.

### Plasmid construction and transformation

For *Escherichia coli* expression vectors, the protein-coding regions of *CPK28* and *APX2* were amplified from tomato cDNA and used to generate recombinant constructs with pET28a and pGEX-4T-1, respectively. Then, the above vectors were introduced into *E. coli* BL21(DE3) strain for protein expression.

To generate the CRISPR-Cas9 vectors, the target sequences of *CPK28* and *APX2* were synthesized according to a web tool of CRISPR-P (available at http://crispr.hzau.edu.cn/CRISPR2/). Each synthesized fragment was annealed and inserted into the AtUb-sgRNA-AtUBQ-Cas9 intermediate vector. The whole cassette was then shuttled between the *Kpn* I/*Hind* III sites of the pCAMBIA1301 vector. Then, the CRISPR-Cas9 vectors were electroporated into *A. tumefaciens* strain GV3101 for generating the CRISPR-Cas9 gene-edited mutants.

For transient overexpression binary vectors, the open reading frames of each gene were amplified based on tomato cDNA and cloned into pDONR-Zeo via Gateway BP reaction (Invitrogen). The point-mutation vectors of APX2 were introduced based on the wild type pDNOR-APX2 by Q5® Site-Directed Mutagenesis Kit (New England Biolabs, E0552). After confirmation with Sanger sequencing, the fragment cassette was shuttled through LR cloning into destination vectors: pGTQL1221YC and pGTQL1211YN for BiFC assay, pCAMBIA-GW-nLUC and pCAMBIA-GW-cLUC for split-Luc assay, pGWB417 with C-terminal MYC tag, pGWB505 with C-terminal GFP tag, respectively. The binary vectors were introduced into *A. tumefaciens* strain GV3101 for transient expression in *N. benthamiana*, and into strain C58C1 for transient expression in tomato. The transient overexpression assays in *N. benthamiana* and tomato plants were performed as previously described (Reichardt et al., 2018).

All primers for the plasmid construction are listed in Supplemental Table S2.

### Thermotolerance and ROS analysis

After high temperature-stress treatments, plant thermotolerance was assessed by quantifying MDA contents (Cheng et al., 2014), relative electrolyte leakage (Pan et al., 2019), chlorophyll fluorescence of the maximum quantum yield of PSII ($F_v/F_m$; Pan et al., 2019), and chlorophyll contents (Liu et al., 2018).

To explore ROS accumulation, DAB and NBT staining were performed to indicate $H_2O_2$ and $O_2^-$ as previously described (Hu et al., 2020) with minor modifications. The tomato leaves were incubated with freshly prepared 1 mg $mL^{-1}$ DAB in 50 mM Tris-HCl (pH 3.8) for 12 h in dark at room temperature, or 0.1 mg $mL^{-1}$ NBT in 25 mM HEPES buffer (pH 7.8) for 2 h. The accumulation of $H_2O_2$ in the leaves was quantified according to the method described previously (Willekens et al., 1997). Briefly, 0.3 g leaf material was ground in 3 mL of 0.2 M $HClO_4$ at 4°C, and the homogenate was centrifuged at 6,000 *g* for 10 min at 4°C. The supernatant was neutralized to pH 6.0 with 4 M KOH, and centrifuged at 6,000 *g* for 10 min at 4°C. The supernatant was loaded onto an AG1x8 prepacked column (Bio-Rad, USA), and the solution was eluted with 4 mL $ddH_2O$. The elute (800 μL) was mixed with 400 μL of reaction buffer containing 4 mM 2,2′-azino-*di*(3-ethylbenzthizoline-6-sulfonic acid) and 100 mM potassium acetate at pH 4.4, 400 μL $ddH_2O$ and 0.25 U of horseradish peroxidase. Then, the $H_2O_2$ content was measured by the changes in absorbance at 412 nm.

### Immunoblotting assays

The oxidized proteins from the soluble protein were evaluated with an OxyBlot Protein Oxidation Detection Kit

(Chemicon International, USA) following the manufacturer's manuals.

The high temperature-responsive proteins were detected by immunoblot analysis with antibodies against cytosolic APX (Agrisera, AS06180), HSP70 (Agrisera, AS08371), and 2-CP (Beijing Protein Innovation). Secondary antibody used subsequently in these analyses was goat anti-rabbit horseradish peroxidase-linked antibody (Cell Signaling Technology, 7074).

## Y2H assay

The tomato cDNA library construction and yeast two-hybrid (Y2H) screening were performed following the manufacturer's protocol (Clontech). The coding sequences of CPK28VK, a constitutively active variant of CPK28, were cloned into pGBKT7 vector as bait and transformed into AH109 yeast strain. For Y2H screening, colonies were directly cultured to SD-Trp-Leu-Ade-His (-T-L-A-H) plates after mating. For the further confirmation of putative positive clones, the mated colonies carrying pGBKT7-CPK28 and pGADT7-APX2 were transferred from SD-T-L plates to SD-T-L-A-H plates with different diluted concentration.

## BiFC and split-Luc assays

For BiFC and split-Luc assays, the pairs of binary constructs carried by *Agrobacterium tumefaciens* GV3101 strains were transiently expressed in leaves of 5-week-old *N. benthamiana* plants. BiFC assays were performed with a Zeiss LSM 780 confocal microscope as described previously (Zhang et al., 2018). For the split-Luc assays, the leaf discs, pre-infiltrated with 15 mM $CaCl_2$, 1.5 mM EGTA, or $dH_2O$ control for 1 h, were then incubated with 100 μL 1mM luciferin (MedChemExpress) solution in a 96-well plate. After 10 min incubation, the protein–protein interaction intensity was evaluated based on the relative light units by the Centro LB 960 Microplate Luminometer (Berthold Technologies, Germany).

## GST pull-down and Co-IP assays

The 6×His- or GST-fused recombinant proteins were expressed in *E. coli* BL21(DE3) strain and purified with Ni-NTA Agarose (Qiagen) or Pierce Glutathione Agarose (Thermo), respectively. For pull-down assays, about 10 μg of GST or GST-APX proteins were pre-incubated with 10 μL glutathione agarose beads in 400 μL pull-down buffer [10 mM Tris-HCl at pH 7.5, 100 mM NaCl, 1 mM β-mercaptoethanol, 1 mM EDTA, 10% glycerol (v/v), with 0.5% Triton X-100 (v/v)] at 4°C for 1 h with gentle shaking. The agarose beads were harvested by centrifugation, and then inoculated with His-CPK28 proteins in 400 μL pull-down buffer at 4°C for 1 h with gentle shaking. Finally, the pulled-down proteins were collected and released from agarose beads by boiling with SDS loading buffer. GST-APX pulled-down proteins were detected by immunoblotting with anti-His antibody (Sigma).

For Co-IP assays, a pair of binary vectors with either an MYC or a GFP tag were co-expressed in *N. benthamiana* leaves. The leaf samples were collected at 2 d post-inoculation, and ground in IP buffer [50 mM Tris-HCl, pH 7.5, 150 mM NaCl, 5 mM EDTA, 0.5% Triton X-100 (v/v); 1× protease inhibitor (Roche), 2.5 μL 0.4 M DTT, 2 μL 1 M NaF, and 2 μL 1 M $Na_3VO_4$ added for 1 mL buffer before using]. Each set of GFP-tagged soluble protein immunoprecipitation was operated in 1 mL IP buffer with 15 μL of anti-GFP agarose beads (Chromotek). After 3 h of gentle shaking at 4°C, the agarose beads were washed 3 times with washing buffer (150 mM NaCl, 50 mM Tris-HCl, pH 7.5, 5 mM EDTA, and 0.1% Triton X-100 [v/v]), and once more with 50 mM Tris-HCl, pH 7.5. Then, the immunoprecipitated proteins were detected by immunoblotting with indicated antibodies.

## LC–MS/MS analysis and phosphorylation assays

The *in vitro* phosphor-sites identification with LC–MS/MS analysis was performed as reported previously (Zhou et al., 2018). Briefly, the phosphorylation reaction dependent on GST-APX2 as the substrate and CPK28-His as the kinase was incubated for 3 h at room temperature. Then, the substrate proteins were separated and collected by SDS-PAGE for further digestion with trypsin overnight. The phosphopeptides were analyzed with LTQ Orbitrap Elite (Thermo-Fisher).

The *in vitro* phosphorylation reactions were performed in 30 μL of kinase buffer (25 mM Tris-HCl, pH 7.5, 10 mM $MgCl_2$, 0.1 mM $CaCl_2$, 1 mM DTT, and 0.2 mM ATP) containing 1 μg CPK28-His and 10 μg of substrate proteins at 25°C with 2 h of gentle shaking. For *in planta* phosphorylation reactions, the indicated binary vectors with either an MYC or a GFP tag were co-expressed in *N. benthamiana* leaves for 2 d, and then the proteins were extracted and incubated in 1 mL IP buffer with 15 μL of anti-MYC agarose beads (Chromotek). After 3 h of gentle shaking at 4°C, the agarose beads were washed 3 times with washing buffer, and once more with 50 mM Tris-HCl, pH 7.5. The immunoprecipitated proteins were released from agarose beads by boiling in SDS loading buffer.

The phosphorylation of recombinant proteins from *in vitro* and *in planta* phosphorylation reactions were analyzed by immunoblotting with anti-pSer/pThr antibody (ECM Biosciences, PM3801) or anti-pThr antibody (Cell Signaling Technology, 9386) after protein separation by SDS-PAGE.

## Measurements of antioxidant contents and enzyme activities

For the antioxidant enzyme activity assays *in planta*, 0.3 g leaf sample was ground with 3 mL ice-cold enzyme buffer [25 mM HEPES, 0.2 mM EDTA, 2 mM AsA, and 2% polyvinylpolypyrrolidone (w/v), pH 7.8]. After 4°C-centrifugation at 12,000 *g* for 20 min, the supernatants were used for the subsequent enzyme activity determination with a SHIMADZU UV-2410PC spectrophotometer (Shimadzu, Japan). The enzyme activities of APX and DHAR were analyzed by a decline in $A_{290}$ and an increase in $A_{265}$, respectively (Nakano and Asada, 1981). CAT activity was

determined according to the consumption of $H_2O_2$ at $A_{240}$ (Veljovic-Jovanovic et al. 2001). GR activity was calculated on the rate of decrease in the absorbance of NADPH at $A_{340}$ (Foyer and Halliwell, 1976). For APX activity assay *in vitro*, *E. coli*-expressed recombinant GST-APX isoforms and GST control were used for the assay by adding sodium ascorbate (ASC) and $H_2O_2$ to final concentration at 0.4 and 1 mM, respectively. After adding $H_2O_2$, the samples were immediately analyzed the changes of the absorbance at $A_{290}$ every 15 s for a 2-min recording time (Yang et al., 2015). Protein concentration was determined by the Bradford method.

For the antioxidant content assays, about 0.1 g leaf sample was ground to powder in liquid nitrogen and extracted into 1 mL 0.2 M HCl. After 4°C-centrifugation at 14,000 *g* for 10 min, the 0.5 mL of supernatant supplement with 100 µL 0.2 M phosphate buffer (pH 5.6) was neutralized with 0.2 M NaOH to pH 4–5. Then, the neutralized extracts were used to measure both ascorbate and glutathione using spectrophotometric assays according to previous methods (Noctor et al., 2016).

### Statistical analysis

At least three independent biological replicates were sampled for each determination. Unless otherwise stated, each biological replicate consisted of an independent sample that was a pool of two leaves, each taken from a different plant. The experiments were independently performed 2–3 times. The obtained data were subjected to analysis of variance using SAS 8.0 software (SAS Institute), and means were compared using Tukey's test at the 5% level.

### Accession numbers

Genetic information from this article can be found in the Sol Genomics Network under the following accession numbers: CPK28, Solyc02g083850; APX2, Solyc06g005150.

## Supplemental data

The following materials are available in the online version of this article.

**Supplemental Figure S1.** $Ca^{2+}$ enhanced plant thermotolerance in tomato.

**Supplemental Figure S2.** Sequence alignment of cytosolic APXs in tomato and Arabidopsis.

**Supplemental Figure S3.** Identification of transiently overexpressed APX2 variants in *apx2* mutants.

**Supplemental Table S1.** List of CPK28-interacting protein candidates identified from Y2H screening.

**Supplemental Table S2.** The primers used in this study.

## Funding

This work was supported by the National Natural Science Foundation of China (31822046, 31772355), the Natural Science Foundation of Zhejiang Province for Distinguished Young Scholar (LR19C150001), the Key Research and Development Program of Zhejiang Province (2021C02040), and the Fundamental Research Funds for the Central Universities. We thank Dr. Youping Xu (Zhejiang University) for assistance with MS analysis.

*Conflict of interest statement.* None declared.

## References

**Athar HUR, Khan A, Ashraf M** (2008) Exogenously applied ascorbic acid alleviates salt-induced oxidative stress in wheat. Environ Exp Bot **63**: 224–231

**Asano T, Tanaka N, Yang GX, Hayashi N, Komatsu S** (2005) Genome-wide identification of the rice calcium-dependent protein kinase and its closely related kinase gene families: comprehensive analysis of the CDPKs gene family in rice. Plant Cell Physiol **46**: 356–366

**Awad J, Stotz HU, Fekete A, Krischke M, Engert C, Havaux M, Berger S, Mueller MJ** (2015) 2-Cysteine peroxiredoxins and thylakoid ascorbate peroxidase create a water-water cycle that is essential to protect the photosynthetic apparatus under high light stress conditions. Plant Physiol **167**: 1592–1603

**Bender KW, Blackburn RK, Monaghan J, Derbyshire P, Menke FLH, Zipfel C, Goshe MB, Zielinski RE, Huber SC** (2017) Autophosphorylation-based calcium ($Ca^{2+}$) sensitivity Priming and $Ca^{2+}$/calmodulin inhibition of *Arabidopsis thaliana* $Ca^{2+}$-dependent protein kinase 28 (CPK28). J Biol Chem **292**: 3988–4002

**Boudsocq M, Sheen J** (2013) CDPKs in immune and stress signaling. Trends Plant Sci **18**: 30–40

**Boudsocq M, Willmann MR, McCormack M, Lee H, Shan LB, He P, Bush J, Cheng SH, Sheen J** (2010) Differential innate immune signalling via $Ca^{2+}$ sensor protein kinases. Nature **464**: 418–422

**Cai HY, Cheng JB, Yan Y, Xiao ZL, Li JZ, Mou SL, Qiu AL, Lai Y, Guan DY, He SL** (2015) Genome-wide identification and expression analysis of calcium-dependent protein kinase and its closely related kinase genes in *Capsicum annuum*. Front Plant Sci **6**: 737

**Campo S, Baldrich P, Messeguer J, Lalanne E, Coca M, San Segundo B** (2014) Overexpression of a calcium-dependent protein kinase confers salt and drought tolerance in rice by preventing membrane lipid peroxidation. Plant Physiol **165**: 688–704

**Chang WJ, Su HS, Li WJ, Zhang ZL** (2009) Expression profiling of a novel calcium-dependent Protein kinase gene, *LeCPK2*, from tomato (*Solanum lycopersicum*) under heat and pathogen-related hormones. Biosci Biotechnol Biochem **73**: 2427–2431

**Cheng F, Yin LL, Zhou J, Xia XJ, Shi K, Yu JQ, Zhou YH, Foyer CH** (2016) Interactions between 2-Cys peroxiredoxins and ascorbate in autophagosome formation during the heat stress response in *Solanum lycopersicum*. J Exp Bot **67**: 1919–1933

**Cheng F, Zhou YH, Xia XJ, Shi K, Zhou J, Yu JQ** (2014) Chloroplastic thioredoxin-f and thioredoxin-m1/4 play important roles in brassinosteroids-induced changes in $CO_2$ assimilation and cellular redox homeostasis in tomato. J Exp Bot **65**: 4335–4347

**Cheng SH, Willmann MR, Chen HC, Sheen J** (2002) Calcium signaling through protein kinases. The Arabidopsis calcium-dependent protein kinase gene family. Plant Physiol **129**: 469–485

**Choudhury FK, Rivero RM, Blumwald E, Mittler R** (2017) Reactive oxygen species, abiotic stress and stress combination. Plant J **90**: 856–867

**Christodoulou J, Malmendal A, Harper JF, Chazin WJ** (2004) Evidence for differing roles for each lobe of the calmodulin-like domain in a calcium-dependent protein kinase. J Biol Chem **279**: 29092–29100

**Ding YF, Cao JM, Ni L, Zhu Y, Zhang AY, Tan MP, Jiang MY** (2013) ZmCPK11 is involved in abscisic acid-induced antioxidant defence and functions upstream of ZmMPK5 in abscisic acid signalling in maize. J Exp Bot **64**: 871–884

**Dubiella U, Seybold H, Durian G, Komander E, Lassig R, Witte CP, Schulze WX, Romeis T** (2013) Calcium-dependent protein

kinase/NADPH oxidase activation circuit is required for rapid defense signal propagation. Proc Natl Acad Sci USA **110**: 8744–8749

**Dubrovina AS, Kiselev KV, Khristenko VS** (2013) Expression of calcium-dependent protein kinase (CDPK) genes under abiotic stress conditions in wild-growing grapevine *Vitis amurensis*. J Plant Physiol **170**: 1491–1500

**Dubrovina AS, Kiselev KV, Khristenko VS, Aleynova OA** (2017) The calcium-dependent protein kinase gene *VaCPK29* is involved in grapevine responses to heat and osmotic stresses. Plant Growth Regul **82**: 79–89

**Foyer CH, Halliwell B** (1976) The presence of glutathione and glutathione reductase in chloroplasts: a proposed role in ascorbic acid metabolism. Planta **133**: 21–25

**Foyer CH, Noctor G** (2011) Ascorbate and glutathione: the heart of the redox hub. Plant Physiol **155**: 2–18

**Fryer MJ, Ball L, Oxborough K, Karpinski S, Mullineaux PM, Baker NR** (2003) Control of *Ascorbate Peroxidase 2* expression by hydrogen peroxide and leaf water status during excess light stress reveals a functional organisation of *Arabidopsis* leaves. Plant J **33**: 691–705

**Gravino M, Savatin DV, Macone A, De Lorenzo G** (2015) Ethylene production in *Botrytis cinerea*- and oligogalacturonide-induced immunity requires calcium-dependent protein kinases. Plant J **84**: 1073–1086

**Hahn A, Bublak D, Schleiff E, Scharf KD** (2011) Crosstalk between Hsp90 and Hsp70 chaperones and heat stress transcription factors in tomato. Plant Cell **23**: 741–755

**Hu Z, Lv X, Xia X, Zhou J, Shi K, Yu J, Zhou Y** (2016) Genome-wide identification and expression analysis of calcium-dependent protein kinase in tomato. Front Plant Sci **7**: 469

**Hu ZJ, Ma QM, Foyer CH, Lei C, Choi HW, Zheng CF, Li JX, Zuo JH, Mao Z, Mei YY, et al.** (2021) High $CO_2$- and pathogen-driven expression of the carbonic anhydrase βCA3 confers basal immunity in tomato. New Phytol **229**: 2827–2843. http://dx.doi.org/10.1111/nph.17087

**Hu ZJ, Sun ZH, Ma QM, Yang XQ, Feng SX, Shao SJ, Shi K** (2020) *N*-decanoyl-homoserine lactone alleviates elevated $CO_2$-induced defense suppression to *Botrytis cinerea* in tomato. Sci Hortic **268**: 109353

**Jang HH, Lee KO, Chi YH, Jung BG, Park SK, Park JH, Lee JR, Lee SS, Moon JC, Yun JW, et al.** (2004) Two enzymes in one: Two yeast peroxiredoxins display oxidative stress-dependent switching from a peroxidase to a molecular chaperone function. Cell **117**: 625–635

**Lamers J, van der Meer T, Testerink C** (2020) How plants sense and respond to stressful environments. Plant Physiol **182**: 1624–1635

**Li CL, Wang M, Wu XM, Chen DH, Lv HJ, Shen JL, Qiao Z, Zhang W** (2016) THI1, a thiamine thiazole synthase, interacts with $Ca^{2+}$-dependent protein kinase CPK33 and modulates the *S*-type anion channels and stomatal closure in Arabidopsis. Plant Physiol **170**: 1090–1104

**Liu CC, Ahammed GJ, Wang GT, Xu CJ, Chen KS, Zhou YH, Yu JQ** (2018) Tomato CRY1a plays a critical role in the regulation of phytohormone homeostasis, plant development, and carotenoid metabolism in fruits. Plant Cell Environ **41**: 354–366

**Liu Y, Xu CJ, Zhu YF, Zhang LN, Chen TY, Zhou F, Chen H, Lin YJ** (2018) The calcium-dependent kinase OsCPK24 functions in cold stress responses in rice. J Integr Plant Biol **60**: 173–188

**Lv XZ, Li HZ, Chen XX, Xiang X, Guo ZX, Yu JQ, Zhou YH** (2018) The role of calcium-dependent protein kinase in hydrogen peroxide, nitric oxide and ABA-dependent cold acclimation. J Exp Bot **69**: 4127–4139

**Maddison J, Lyons T, Plochl M, Barnes J** (2002) Hydroponically cultivated radish fed L-galactono-1,4-lactone exhibit increased tolerance to ozone. Planta **214**: 383–391

**Mittler R, Blumwald E** (2010) Genetic engineering for modern agriculture: challenges and perspectives. Annu Rev Plant Biol **61**: 443–462

**Mittler R, Finka A, Goloubinoff P** (2012) How do plants feel the heat? Trends Biochem Sci **37**: 118–125

**Monaghan J, Matschi S, Shorinola O, Rovenich H, Matei A, Segonzac C, Malinovsky FG, Rathjen JP, MacLean D, Romeis T, Zipfel C** (2014) The calcium-dependent protein kinase CPK28 buffers plant immunity and regulates BIK1 turnover. Cell Host Microbe **16**: 605–615

**Nakano Y, Asada K** (1981) Hydrogen-peroxide is scavenged by ascorbate-specific peroxidase in spinach-chloroplasts. Plant Cell Physiol **22**: 867–880

**Noctor G, Mhamdi A, Foyer CH** (2016) Oxidative stress and antioxidative systems: recipes for successful data collection and interpretation. Plant Cell Environ **39**: 1140–1160

**Ohama N, Sato H, Shinozaki K, Yamaguchi-Shinozaki K** (2017) Transcriptional regulatory network of plant heat stress response. Trends Plant Sci **22**: 53–65

**Pan CZ, Zhang H, Ma QM, Fan FJ, Fu RS, Ahammed GJ, Yu JQ, Shi K** (2019) Role of ethylene biosynthesis and signaling in elevated $CO_2$-induced heat stress response in tomato. Planta **250**: 563–572

**Queval G, Hager J, Gakiere B, Noctor G** (2008) Why are literature data for $H_2O_2$ contents so variable? A discussion of potential difficulties in the quantitative assay of leaf extracts. J Exp Bot **59**: 135–146

**Reichardt S, Repper D, Tuzhikov AI, Galiullina RA, Planas-Marques M, Chichkova NV, Vartapetian AB, Stintzi A, Schaller A** (2018) The tomato subtilase family includes several cell death-related proteinases with caspase specificity. Sci Rep **8**: 10531

**Rossel JB, Walter PB, Hendrickson L, Chow WS, Poole A, Mullineaux PM, Pogson BJ** (2006) A mutation affecting *ASCORBATE PEROXIDASE 2* gene expression reveals a link between responses to high light and drought tolerance. Plant Cell Environ **29**: 269–281

**Ruggieri V, Calafiore R, Schettini C, Rigano MM, Olivieri F, Frusciante L, Barone A** (2019) Exploiting genetic and genomic resources to enhance heat-tolerance in tomatoes. Agronomy **9**: 22

**Saijo Y, Hata S, Kyozuka J, Shimamoto K, Izui K** (2000) Overexpression of a single $Ca^{2+}$-dependent protein kinase confers both cold and salt/drought tolerance on rice plants. Plant J **23**: 319–327

**Smirnoff N, Arnaud D** (2019) Hydrogen peroxide metabolism and functions in plants. New Phytol **221**: 1197–1214

**Suzuki N, Miller G, Sejima H, Harper J, Mittler R** (2013) Enhanced seed production under prolonged heat stress conditions in Arabidopsis thaliana plants deficient in cytosolic ascorbate peroxidase 2. J Exp Bot **64**: 253–263

**Veljovic-Jovanovic SD, Pignocchi C, Noctor G, Foyer CH** (2001) Low ascorbic acid in the *vtc-1* mutant of arabidopsis is associated with decreased growth and intracellular redistribution of the antioxidant system. Plant Physiol **127**: 426–435

**Vu LD, Gevaert K, De Smet I** (2019) Feeling the heat: Searching for plant thermosensors. Trends Plant Sci **24**: 210–219

**Wang ML, Li QH, Sun K, Chen X, Zhou QQ, Li H, Zhang XY, Li XH** (2018) Involvement of CsCDPK20 and CsCDPK26 in regulation of thermotolerance in tea plant (*Camellia sinensis*). Plant Mol Biol Rep **36**: 176–187

**Willekens H, Chamnongpol S, Davey M, Schraudner M, Langebartels C, VanMontagu M, Inze D, VanCamp W** (1997) Catalase is a sink for $H_2O_2$ and is indispensable for stress defence in $C_3$ plants. EMBO J **16**: 4806–4816

**Xu XW, Liu M, Lu L, He M, Qu WQ, Xu Q, Qi XH, Chen XH** (2015) Genome-wide analysis and expression of the calcium-dependent protein kinase gene family in cucumber. Mol Genet Genomics **290**: 1403–1414

**Yang H, Mu J, Chen L, Feng J, Hu J, Li L, Zhou JM, Zuo J** (2015) *S*-nitrosylation positively regulates ascorbate peroxidase activity during plant stress responses. Plant Physiol **167**: 1604–1615

**Zhang H, Hu ZJ, Lei C, Zheng CF, Wang J, Shao SJ, Li X, Xia XJ, Cai XZ, Zhou J, et al.** (2018) A plant phytosulfokine peptide

initiates auxin-dependent immunity through cytosolic $Ca^{2+}$ signaling in tomato. Plant Cell **30**: 652–667

**Zhang HF, Liu DY, Yang B, Liu WZ, Mu BB, Song HX, Chen BY, Li Y, Ren DT, Deng HQ, Jiang YQ** (2020) Arabidopsis CPK6 positively regulates ABA signaling and drought tolerance through phosphorylating ABA-responsive element-binding factors. J Exp Bot **71**: 188–203

**Zheng YB, Lyons T, Ollerenshaw JH, Barnes JD** (2000) Ascorbate in the leaf apoplast is a factor mediating ozone resistance in *Plantago major*. Plant Physiol Biochem **38**: 403–411

**Zhou J, Wang X, He Y, Sang T, Wang P, Dai S, Zhang S, Meng X** (2020) Differential phosphorylation of the transcription factor WRKY33 by the protein kinases CPK5/CPK6 and MPK3/MPK6 cooperatively regulates camalexin biosynthesis in Arabidopsis. Plant Cell **32**: 2621–2638

**Zhou JG, Liu DR, Wang P, Ma XY, Lin WW, Cheng SX, Mishev K, Lu DP, Kumar R, Vanhoutte I, et al.** (2018) Regulation of Arabidopsis brassinosteroid receptor BRI1 endocytosis and degradation by plant U-box PUB12/PUB13-mediated ubiquitination. Proc Natl Acad Sci USA **115**: E1906–E1915

**Zhu SY, Yu XC, Wang XJ, Zhao R, Li Y, Fan RC, Shang Y, Du SY, Wang XF, Wu FQ, et al.** (2007) Two calcium-dependent protein kinases, CPK4 and CPK11, regulate abscisic acid signal transduction in Arabidopsis. Plant Cell **19**: 3019–3036

**Zou JJ, Li XD, Ratnasekera D, Wang C, Liu WX, Song LF, Zhang WZ, Wu WH** (2015) Arabidopsis CALCIUM-DEPENDENT PROTEIN KINASE8 and CATALASE3 function in abscisic acid-mediated signaling and $H_2O_2$ homeostasis in stomatal guard cells under drought stress. Plant Cell **27**: 1445–1460

**Zou JJ, Wei FJ, Wang C, Wu JJ, Ratnasekera D, Liu WX, Wu WH** (2010) Arabidopsis calcium-dependent protein kinase CPK10 functions in abscisic acid- and $Ca^{2+}$-mediated stomatal regulation in response to drought stress. Plant Physiol **154**: 1232–1243